IEEE J. Sel. Top. Quantum Electron., Vol. 6, No. 3 (2000) 522-527

Laser-Action in V-Groove-Shaped InGaAs/InP Single Quantum Wires

D. Piester, P. Bönsch, T. Schrimpf, H.-H. Wehmann, A. Schlachetzki

Abstract-- **We report on the realization of a V-groove-shaped single quantum wire laser in the material system InGaAsP/InP. First, we discuss a new laser concept which makes use of a semi-insulating current-blocking layer and InGaAsP waveguiding layers. Simulations demonstrate the concentration of both the current as well as the optical field in the active region. We developed a two-step wet-chemical etching process, to form high quality V-grooves into a layer stack consisting of InP and InGaAsP. By employing anisotropic wet-chemical etching and anisotropic metal-organic vapor-phase epitaxial growth, we demonstrate the feasibility of this concept. We show laser action originating from a single InGaAs quantum wire realized in this concept. The source of a second laser line measured with electroluminescence spectroscopy is discussed.**

Index Terms-- **InP, MOVPE, quantum wire laser, V-groove, wet-chemical etching**

I. INTRODUCTION

During the last decade low-dimensional semiconductor structures find wide applications in optoelectronic devices. A prominent example is their use as active regions in lasers. Quantum structure lasers are expected to show improved device properties such as low threshold current, high optical gain [1], and low temperature sensivity [2]. Thus they are of special interest for monolithic integration with multi-laser applications and low-power electronics.

The advantageous features of quantum wires (QWRs) are enhanced as compared to quantum wells (QWLs) with their quantum confinement in only one dimension. On the other hand quantum dots (QDs) being confined in three dimensions should be superior to QWRs, but such structures are commonly realized by self-organized epitaxial growth [3],[4],[5]. Thus they are statistically distributed in size and area. Eluding this statistical growth, QWRs can be formed in a well-controlled manner just as QWLs by pursuing suitable concepts. Further, the capability of growing lattice matched QWRs offers an additional degree of freedom in structural design and material selection.

Up to now, many efforts have been devoted to the realization of QWR lasers. An example is the use of self-organized growth[6],[7]. In the case of GaAs/AlGaAs QWRs the growth was carried out by molecular beam epitaxy on (775)B-orientated substrates. A comparison with a similar quantum well structure shows that the threshold current of the QWR laser is by far smaller than that of the quantum well laser [6]. Additional possibilities are the growth on a ridge structure [8], the growth on multiatomic steps [9], or the structuring of QWRs by means of electron beam lithography [10]. All these works require particularly demanding technological processes or are based on lattice mismatch.

A further important method is the anisotropic growth on V-groove patterned substrates [11]. Promising is the design published by Toda et al. [12], comprising a QWR DFB laser in the InAsP/InP system. In this case, mass transport of group III

Manuscript received September 15, 1999. This work was supported by the Volkswagen-Stiftung and by the Deutsche Forschungsgemeinschaft.

The authors are with the Institute for Semiconductor Technology, Technical University Carolo-Wilhelmina, Hans-Sommer-Str. 66, D-38106 Braunschweig, Germany.

elements during growth is purposefully used. Up to now, the lowest threshold current measured with a QWR laser is 188 µA at room temperature [13]. This was achieved in the V-groove concept with an InGaAs QWR on GaAs substrate.

Most QWR lasers on patterned substrates were grown on GaAs with GaAs/AlGaAs [14],[15] and InGaAs/AlGaAs [13] layers with emission wavelengths of about 840 nm and 980 nm, respectively. This wavelength range extending even up to 1.3 μm can also be covered by InGaAs/GaAs QDs [5]. However, only In(Ga)As(P)/InP has been experimentally demonstrated for lasers in the 1.55 µm wavelength region [7],[12]. But in comparison with AlGaAs, which is nearly lattice-matched for all compositions to a GaAs substrate, the composition of InGaAs(P) must be controlled very precisely to avoid crystal defects. Another problem is the mass transport during the heating phase before epitaxial growth. This causes rounded V-groove tips resulting in wider QWRs [16]. On the other hand, reproducible high quality InGaAs/InAlAs QWRs were fabricated, making use of the "resharpening" of the Al-containing barriers [17]. However, Al-free structures promise a better longterm stability [18].

QWRs in V-grooves as the active region in lasers require an effective current confinement. This is achieved by *pn*-junctions [19] or by proton implantation [20].

In this paper we present an InGaAsP/InP V-groove laser with an InGaAs single QWR active region grown by metal-organic vapor-phase epitaxy (MOVPE). We clearly demonstrate that a single QWR suffices for laser emission so that we do not have to have recourse to a multiple wire arrangement. For current blocking we use semi-insulating (s. i.) InP. Furthermore, the QWR is embedded in quaternary waveguiding layers. We report on the laser concept and give evidence for its functioning by simulations. We describe the fabrication process of this structure and demonstrate laser action from a single InGaAs QWR. Finally, we discuss the origin of a second laser line which is observed in this structure.

II. Device Structure and Optical Recombination

Figure 1 shows the schematic cross-section of the V-groove QWR laser in the material system InGaAsP/InP. Deposited on n^+-doped InP substrate the first epitaxial layer stack consists of an n-doped InGaAsP layer and an s. i. InP layer. Subsequently, V-grooves are anisotropically etched with standard photolithographic technique into these layers. With this technique it is possible to transform micrometer sizes to the nanometer scale at the V-groove tip. Then in a second epitaxial growth the undoped InGaAs QWR is deposited into the tip of the V-groove. The active region (QWR) is covered by an undoped InGaAsP layer. This layer is followed by a *p*-doped InP layer and covered by a highly *p*-doped InGaAs contact layer. Metal contact stripes are patterned on the top of the structure and on the whole backside. The laser resonator is formed by $(01\bar{1})$ cleavage planes perpendicular to the QWR.

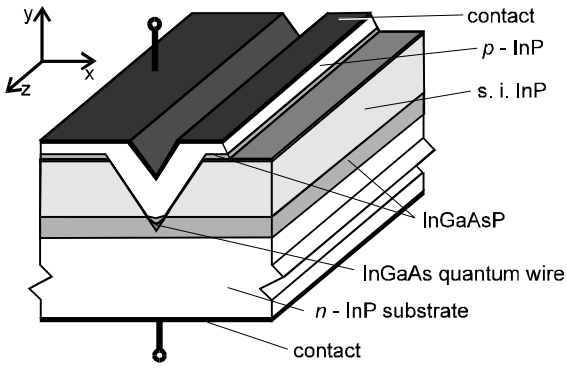

Fig. 1 Structure of QWR laser in InP substrate with V-shaped groove.

The quaternary layers around the quantum wire form an optical waveguide improving the optical confinement factor. Semi-insulating material on both sides of the V-groove provides current blocking which leads the carriers towards the QWR. Shunt connections are minimized in this way.

In order to verify this concept, we calculated the optical recombination rate by the finite-element method employing the program package ToSCA [21]. Figure 2 shows the distribution of the optical recombination rate for the two-dimensional geometrical structure shown in the *x*-*y*-plane. For a better visualization only the vicinity of the active region is shown as a detail of the whole laser structure. In order to obtain optical recombination both electron and hole concentration must be sufficiently high. Due to an efficient current carrier focussing on the actice region enforced by the s. i. InP, the highest recombination rate is found at the QWR location in the tip of the V-groove where electron and hole concentrations have their maxima. The simulation also shows a much reduced, though noticeable optical recombination in the adjacent InGaAsP waveguiding layers. In comparison with the InGaAs QWR the recombination rate is 40 times less due to the reduced electron and hole concentrations in this region.

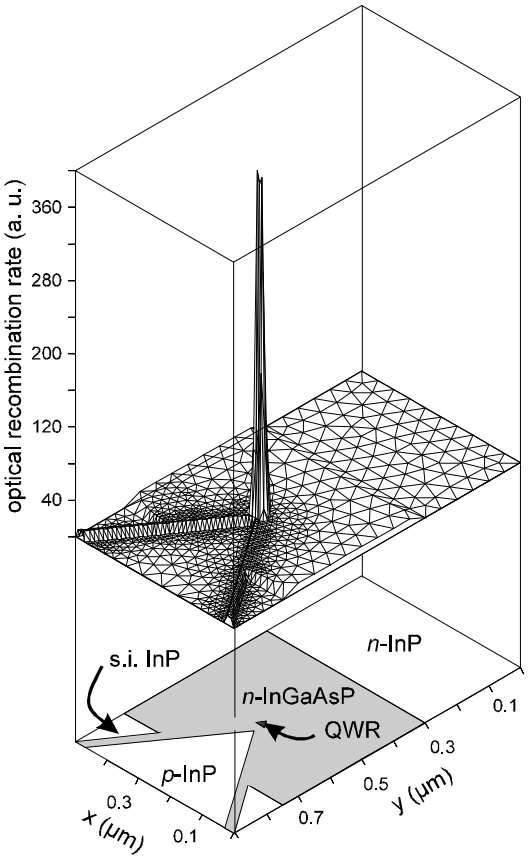

Fig. 2 Numerical simulation of the optical recombination rate within the core region around the quantum wire (cf. Fig. 1).

The waveguiding properties of the InGaAsP layers with a bandgap energy corresponding to 1.2 μm wavelength were calculated using the beam propagation method [22] with an exciting Gaussian beam. Figure 3 shows the distribution of the amplitude of the electric field of the TE fundamental mode as a grey shaded plot of the cleavage plane. High intensities are shown dark, low ones bright. The QWR is superimposed as a black structure in the center. The filling factor of this structure with respect to the QWR is 0.1 %.

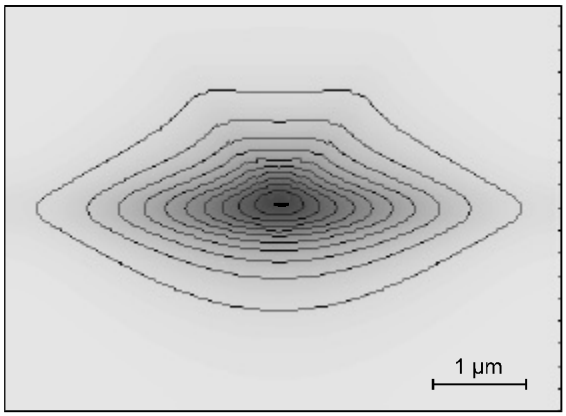

Fig. 3 Distribution of the amplitude of the electric field of the TE-fundamental mode. The curves are isolines of the field intensity.

III. Device Fabrication

We employ a two step MOVPE process on an S-doped InP substrate ($N_D \approx 6 \times 10^{18}$ cm^{-3}) with $(100) \pm 0.5°$ orientation and polished surface finish. The samples are chemically cleaned in boiling propanol, followed by a 5 min etching step in H_2SO_4:H_2O:H_2O_2 (5:1:1) and a thorough rinsing in deionized water.

For MOVPE growth we use a horizontal reactor with IR-heated susceptor. As sources we employed trimethylindium and trimethylgallium as group-III precursors and arsine and posphine as group-V precursors, respectively. For doping sources SiH_4, $(C_5H_5)_2Zn$ and $(C_5H_5)_2Fe$ are used for *n*- and *p*-type as well as s. i. layers,

respectively. Hydrogen is the carrier gas. The total gas flow for all layers is approximately 8000 sccm. Growth temperature and total pressure are 640 °C and 20 hPa, respectively.

We start the growth with a 500 nm thick InP buffer layer (Si-doped, $N_D = 5 \times 10^{17}$ cm^{-3}). Subsequently, the lower InGaAsP waveguiding layer (Si-doped, $N_D = 5 \times 10^{17}$ cm^{-3}) and the s. i. InP current blocking layer (Fe-doped, $N = 5 \times 10^{16}$ cm^{-3}) are deposited.

The growth process is interrupted for etching of the V-grooves. A 40 nm electron-beam evaporated Ti film is used as an etching mask. Between 3 and 4 μm wide stripes in [$01\bar{1}$] direction are formed by lift-off technique [23]. This step requires only conventional optical lithography as opposed to electron beam lithography or ion implantation in other cases [10],[20]. Prior to the Ti evaporation the samples were treated in an oxygen plasma for 20 s in order to remove photoresist residues [24].

A two step wet chemical etching process is used to fabricate high quality V-grooves with {111}A sidewalls. During the first step HBr (37 %) is applied for 30 s which is highly anisotropic for InP. In conjunction with the very low undercutting of the Ti-mask this self-limiting process forms V-grooves in InP with {111} sidewalls with a high pattern fidelity. The etching process is selflimited when the tip of the V-groove is formed. Its depth is only determined by the aperture of the Ti mask. This is shown by the open squares in Fig. 4. However, HBr does not attack InGaAsP so that the depth is stagnent if the width of Ti mask is large enough. The second etching step is performed for 5 s in $HBr:CH_3COOH:K_2Cr_2O_7$ (2:2:1) (BCK for short). Since the etching behaviour of BCK for InGaAsP and InP is nearly the same, it is used to give the V-grooves their final shape. Beyond this the {111} sidewalls, showing ripples on their surfaces after the first etching step, are smoothened [25].

The tip-positions of the V-grooves with different mask openings after this second etching step is marked by the solid squares in Fig. 4. For a width of 3.6 μm the V-groove penetrates the whole s. i. InP top layer (light grey) and ends just in the center of the underlying 400 nm thick quaternary waveguiding layer (dark grey). This optimum case is shown in the two inserts in the lower left corner where the cleaved V-grooves are depicted as scanning electron micrographs (SEM). In the right one the InGaAsP is selectively etched by citric acid:H_2O_2 (7:1) [26] to visualize the material contrast. This leads to an edge on the {111} plane at the interface, whereas in the left picture there is no discontinuity observable. Clearly visible in both pictures is the undercutting of the Ti mask during the second etching step. This is due to the isotropic etching behaviour of BCK. Thus, this step is not self-limiting leading to the deviation of the solid squares from the open ones of the first step in Fig. 4. Nevertheless, this figure clearly demonstrates, that it is possible to adjust the depth of the V-grooves in a controlled manner by the width of the Ti mask aperture.

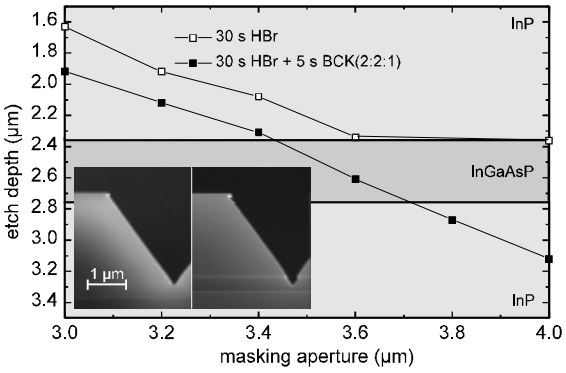

Fig. 4 Etch depth in an InP/InGaAsP layer stack in dependence of the Ti masking aperture.

Prior to the second epitaxial step the patterned samples were etched in HF (5 %, 10 s) and $H_2SO_4:H_2O$ (5:1, 1 min). As compared to the first cleaning step, we omitted H_2O_2 in order to prevent the appearance of {311} surfaces in the vicinity of the tip of the V-groove. To reduce the In mass transport, the first three layers, i. e.

nominally 50 nm InP, 5 nm $In_{0.53}Ga_{0.47}As$ and 20 nm InP were grown at 600 °C and 100 hPa. This forms a nearly lattice-matched InGaAs QWR in the tip of the V-groove [27]. Extending the growth of bare QWRs, we employ additional layers required for a laser structure. These layers were grown with standard parameters (640 °C, 20 hPa). During temperature increase the growth of a 20 nm thick InP layer is carried out in order to provide stable conditions. Covering the active region, the quaternary layer, the *p*-doped InP layer (cf. Fig. 1) and a p^+-doped InGaAs contact layer are grown.

After the growth, Ti-AuGe-Au is electron-beam deposited on the p^+-InGaAs top layer for the p-side ohmic contact. By means of standard photolithography 100 µm wide mesa-stripes are etched by using BCK. Finally, the sample is lapped from the backside down to about 100 μm. Ti-AuGe-Au is deposited to form the *n*-side ohmic contact. The samples are cleaved as laser bars of about 1 mm resonator length. The laser bars are fixed onto a Cu-holder by indium. The electrical contacts are bonded.

Figure 5 shows a SEM picture of a mirror of such a device which was etched in citric acid:H_2O_2 (7:1) in order to obtain a material contrast. Due to the material-selective overetching the QWR region is clearly visible. Its actual dimensions are 5.5×180 nm^2 [28].

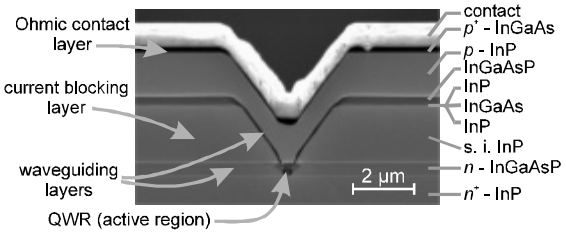

Fig. 5 Scanning-electron micrograph of a cleaved structure after material-selective etching.

IV. Results

At room temperature we measured the near-field of the devices by means of an infra-red microscope supplied with a PbS-vidikon camera. A filter with long wavelength transmittance above 1100 nm is used to suppress short wavelength radiation. In Fig. 6 the near field is shown for a cw current of 80 mA. The voltage across the device is about 1.1 V. The contour plot corresponds to the electroluminescence (EL) intensity of a single QWR. The highest intensity in the center of the picture is located at the V-groove's tip. This is proven by superimposing the optical image with additional illumination of the cleavage plane. The measurement is in good agreement with the simulation of the optical recombination plot shown in Fig. 2. This experimental finding clearly demonstrates that the s. i. InP layer concentrates very efficiently the current into the QWR.

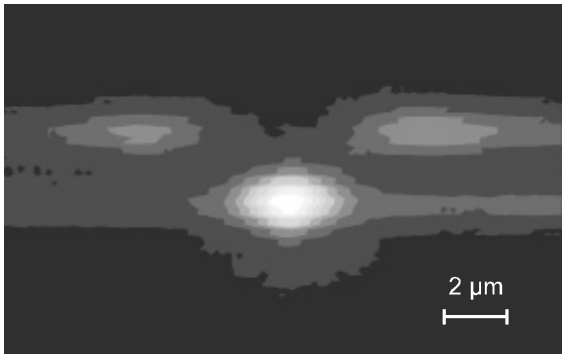

Fig. 6 Optical near field measured with an microscope supplied with an PbS-vidikon camera.

Additional maxima are visible, which are located in the quaternary layers grown on the (100) top surface at the edges of the V-groove. The embedding by InP (cf. Fig. 3) forms waveguides at the edges. This is probably the reason for observing EL intensity at these locations.

The same argument applies to the lower quaternary layer on both sides of the QWR. The distribution of the intensity shows a distinct anisotropy with respect to the *x*- and *y*-axis, respectively. This is in good agreement with the results of the simulation (see Fig. 3).

Beyond the near field, the EL spectra were examined at 15 K by means of a closed-cycle He-cryostat. We used a conventional setup with Peltier-cooled Ge detector and

monochromator with a focal length of 640 mm with lock-in technique. Electrical excitation by quasi-continuous pulses of 100 μs duration with a duty cycle of 30 % are employed in order to reduce the thermal load.

Four spectra corresponding to four different currents ranging from 200 to 460 mA are displayed in Fig. 7. In the low current regime three peaks are visible. As demonstrated by the PL-study on InGaAs/InP quantum wires [27], the peak at 890 meV can be assigned to the QWR. The peak at 1066 meV originates from the quaternary material. This is corroborated by accompanying EL-investigations with a sample consisting of a single quantum well embedded in quaternary material as well as with the QWR-laser structure. In its low-energy shoulder there is a peak shifted by 40 meV which is probably due to an electron acceptor transition in the upper quaternary layer. This may be related to an out-diffusion of Zn from the p-doped InP layer. Furthermore, a signal is visible at an energy of 928 meV. This signal originates from the thin quantum well which is formed on the {111} sidewalls [28]. With higher currents the intensity of this peak increases only slightly, and no stimulated emission is recognized. On the other hand the QWR- and InGaAsP-related peaks increase in intensity and simultaneously become narrower above 350 mA, which we attribute to laser action. These arguement clearly prove that the (100) QWL at the substrate surface is not optically active.

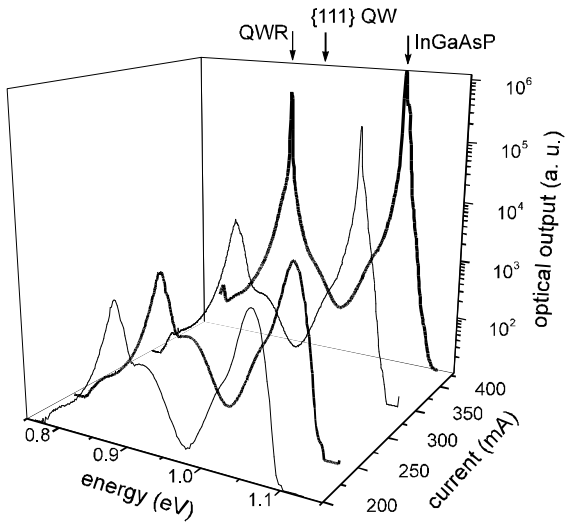

Fig. 7 Electroluminescence spectra of the structure of Fig. 5 for different driving currents as a parameter. The abscissa is the photon energy.

It follows from the spectra that there are two concurrent wavelength regions concurrently emitting stimulated radiation. The optical power-current curves as measured separately for each of the two main peaks elucidate this fact. We measured the optical power measured in a wavelength interval of 9 nm around the maxima as displaced in Fig. 8. For lower currents the device behaves like an LED and the intensity increases, due to spontaneous recombination. Laser action starts with the onset of stimulated emission at the threshold current. Two typical spectra for currents above threshold are represented in the upper part of Fig. 8. Their comb-like shape is typical for lasers with Fabry-Perot resonator. The individual peaks represent the longitudinal modes. Their wavelength separation is inversely proportional to the resonator length.

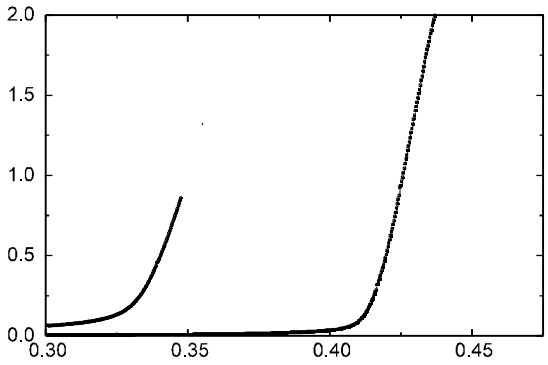
2.0
1.5
1.0
0.5
0.0
0.30
0.35
0.40
0.45

VII. REFERENCES

[1] M. Asada, Y. Miyamoto, and Y. Suematsu, "Gain and the Threshold of Three-Dimensional Quantum-Box Lasers", *IEEE J. Quantum Electron.*, vol. QE-22, pp. 1915-1921, 1986.

[2] Y. Arakawa and H. Sakaki, "Multidimensional quantum well laser and temperature dependence of its threshold current", *Appl. Phys. Lett.*, vol. 40, pp. 939-941, 1982.

[3] N. N. Ledentsov, "Quantum dot lasers: the birth and future trends", *Semiconductors*, vol. 33, pp. 946-950, 1999.

[4] W. Zhou, O. Qasaimeh, J. Phillips, S. Krishna, and P. Bhattacharya, "Bias-controlled wavelength switching in coupled-cavity $In_{0.4}Ga_{0.6}As$/GaAs self-organized quantum dot lasers", *Appl. Phys. Lett.*, vol. 74, pp.783-785, 1999.

[5] G. Park, O. B. Shchekin, S. Csutak, D. L. Huffaker, and D. G. Deppe, "Room-temperature continuous-wave operation of a single-layered 1.3 µm quantum dot laser", *Appl. Phys. Lett.*, vol. 75, pp. 3267-3269, 1999.

[6] M. Higashiwaki, S. Shimomura, S. Hiyamizu, and S. Ikawa, "Self-organized GaAs quantum-wire lasers grown on (775)*B*-oriented GaAs substrates by molecular beam epitaxy", *Appl. Phys. Lett.*, vol. 74, pp. 780-782, 1999.

[7] S. T. Chou, D. E. Wohlert, K. Y. Cheng, and K. C. Hsieh, "The directionality of quantum confinement on strain-induced quantum-wire lasers", *J. Appl. Phys.*, vol. 83, pp. 3469-3472, 1998.

[8] S. Watanabe, S. Koshiba, M. Yoshita, H. Sakaki, M. Baba, and H. Akiyama, "Stimulated emission in ridge quantum wire laser structures measured with optical pumping and microscopic imaging methods", *Appl. Phys. Lett.*, vol. 73, pp. 511-513, 1998.

[9] S. Hara, J. Motohisa, and T. Fukui, "Self-organised InGaAs quantum wire lasers on GaAs multi-atomic steps", *Electron. Lett.*, vol. 34, pp. 894-895, 1998.

[10] T. Kojima, M. Tamura, H. Nakaya, S. Tanaka, S. Tamura, and S. Arai, "GaInAsP/InP Compressively Strained Quantum-Wire Lasers Fabricated by Electron Beam Lithography and 2-Step Organometallic Vapor Phase Epitaxy", *Jpn. J. Appl. Phys.*, vol. 37, pp. 4792-4800, 1998.

[11] M. Ishikawa, W. Pan, Y. Kaneko, H. Yaguchi, K. Onabe, R. Ito, Y. Shiraki, "Polarization Characteristics of Crescent-Shaped Tensile-Strained GaAsP/AlGaAs Quantum Wire-Like Lasers", *Jpn. J. Appl. Phys.*, vol. 37, pp. 1556-1558, 1998.

[12] T. Toda, Y. Nakano, "Room Temperature Operation of 1.5 µm InAsP/InP Strained Quantum Wire DFB Lasers Fabricated by Mass Transport Method", *Proc. of 11th International Conference on Indium Phosphide and Related Materials*, pp. 17-20, 16-20 May 1999, Davos, Switzerland.

[13] S. Tiwari, G. D. Pettit, K. R. Milkove, F. Legoues, R. J. Davis, and J. M. Woodall, "High efficiency and low threshold current strained V-groove quantum-wire lasers", *Appl. Phys. Lett.*, vol. 64, pp. 3536-3538, 1994.

[14] S. Simhony, E. Kapon, E. Colas, D. M. Hwang, N. G. Stoffel, and P. Worland, "Vertically stacked multiple-quantum-wire semiconductor diode lasers", *Appl. Phys. Lett.*, vol. 59, pp. 2225-2227, 1991.

[15] T. G. Kim, X.-L. Wang, K. Komori, K. Hikosaka, and M. Ogura, "AlGaAs/GaAs quantum wire lasers fabricated by flow rate modulation epitaxy", *Electron. Lett.*, vol. 35 pp. 639-640, 1999.

[16] P. Bönsch, D. Wüllner, T. Schrimpf, H.-H. Wehmann, and A. Schlachetzki, "Growth of InGaAs/InP quantum wires on patterned substrates", *7th European Workshop on Metal-Organic Vapor Phase Epitaxy and Related Growth Techniques (EW-MOVPE VII)*, June 8-11, Berlin, Germany, C1, 1997.

[17] M. Kappelt, M. Grundmann, A. Krost, V. Türck, and D. Bimberg, "InGaAs quantum wires grown by low pressure metalorganic chemical vapor deposition on InP V-grooves", *Appl. Phys. Lett.*, vol. 68, pp. 3596-3598, 1996.

[18] J. Diaz, H. J. Yi, M. Razeghi, G. T. Burnham, "Long-term reliability of Al-free InGaAsP/GaAs (λ = 808 nm) lasers at high-power high-temperature operation", *Appl. Phys. Lett.*, vol. 71, pp. 3042-3044, 1997.

[19] T. G. Kim, K. H. Park, S.-M. Hwang, Y. Kim, E. K. Kim, S.-K. Min, S.-J. Leem, J.-I. Jeon, J.-H. Park, W. S. C. Chang, "Performance of GaAs-AlGaAs V-Grooved Inner Stripe Quantum-Well Wire Lasers with Different Current Blocking Configurations, *IEEE J. Quantum Electron.*, vol. 34, pp. 1461-1468, 1998.

[20] E. Kapon, S. Simhony, R. Bhat, and D. M. Hwang, "Single quantum wire semiconductor lasers", *Appl. Phys. Lett.*, vol. 55, pp. 2715-2717, 1989.

[21] "ToSCA Two-Dimensional Semi-Conductor Analyse Package", Weierstraß-Institut, Berlin, Germany

[22] "BPM_CAD Waveguide Optics Modelling Software System", Optiwave Corporation, Nepean, Ontario, Canada

[23] R. Klockenbrink, E. Peiner, H.-H. Wehmann, and A. Schlachetzki, "Wet Chemical Etching of Alignment V-Grooves in (100) InP through Titanium or $In_{0.53}Ga_{0.47}As$ Masks", *J. Electrochem. Soc.*, vol. 141, pp. 1594-1599, 1994.

[24] H.-H. Wehmann, T. Schrimpf, P. Bönsch, D. Wüllner, D. Piester, A. Schlachetzki, and R. Lacmann, "Growth and characterization of InGaAs quantum-wires", *Third International Workshop on Heterostructure Epitaxy and Devices (HEAD'97)*, edited by P. Kordos and J. Novak, NATO Series 3/48 (Kluwer Academic, Dordrecht), pp.199-202, 1998.

[25] P. Bönsch, D. Wüllner, T. Schrimpf, A. Schlachetzki, and R. Lacmann, "Ultrasmooth V-Grooves in InP by Two-Step Wet Chemical Etching", *J. Electrochem. Soc.*, vol. 145, pp. 1273-1276, 1998.

[26] H.-H. Wehmann and A. Schlachetzki, "Technology and Characterization of a Photoconductive device on InP", *ESSDERC'89*, edited by A. Heuberger, H. Ryssel, P. Lange, Springer, Berlin, pp. 491-494, 1989.

[27] T. Schrimpf, P. Bönsch, D. Wüllner, H.-H. Wehmann, A. Schlachetzki, F. Bertram, T. Riemann, and J. Christen, "InGaAs quantum wires and wells on V-grooved InP substrates", *J. Appl. Phys.*, vol. 86, pp. 5207-5214, 1999.

[28] T. Schrimpf, D. Piester, H.-H. Wehmann, P. Bönsch, D. Wüllner, A. Schlachetzki, C. Mendorf, und H. Lakner, "Preparation and Characterization of InGaAs Quantum Wires on V-Groove Patterned InP", *Proc. of 11th International Conference on Indium Phosphide and Related Materials*, pp. 507-510, 16-20 May 1999, Davos, Switzerland.

[29] S. M. Sze, "Physics of Semiconductor Devices", 2nd Edition, *John Wiley & Sons*, New York, 1981.